

Abscission occurred in a markedly different manner: A very extensive stretching of the intercellular bridge between the daughter cells could be observed. In these cells, the midbody itself apparently never disassembled [Web movie 3, part 3 (11)]. We conclude that a key parameter for the movement of the mother centriole, and for abscission, is cellular adhesion to the substrate or contact to neighboring cells.

Strongly adherent cultured cells can apparently divide by traction-mediated "cytofission" (21). Some mammalian cells can divide without actomyosin rings when attached to a solid substrate (22), a behavior reminiscent of *Dictyostelium discoideum* cytokinesis mutants (23). Traction-mediated cytofission is unlikely to occur in a tissue where cells are not free to move far away from one another and thus could be an artifact due to cell culture on too-adhesive substrates rather than a genuine alternative pathway. We noted, for example, that 3T3 or L929 cells grown on a very adherent substrate show many binucleated cells, suggesting frequent cytokinesis defects. Moreover, several recent reports have shown that cytokinesis can reverse after furrowing, leading to the formation of binucleated cells, or it can be blocked at a late stage, the two cells being linked by a cytoplasmic bridge (24, 25). In agreement with other reports (26–28), our data strongly support the idea that abscission is a regulated process.

Our observations on living cells can be interpreted by the model shown in Fig. 4. At the exit of metaphase, cells assemble three structures: the so-called central spindle, the cleavage furrow, and the telophase disk/midbody. We propose that the disassembly of the central spindle and the cleavage furrow, both necessary for abscission, are distinct events that, like metaphase spindle disassembly, are under tight control; we also propose that these controls would involve the repositioning of the centrosome with respect to the midbody.

This control implies that the centrosome, which normally maintains itself at the cell center, moves transiently to the cell periphery. In addition to its relevance for cell division control, such a behavior could reveal a more general function of the centrosome, namely to integrate spatial constraints, for example, during cell locomotion and cell differentiation.

References and Notes

1. L. H. Hartwell, T. A. Weinert, *Science* **246**, 629 (1989).
2. A. W. Murray, *Nature* **359**, 599 (1992).
3. L. Hartwell, *Cell* **71**, 543 (1992).
4. M. A. Hoyt, *Cell* **102**, 267 (2000).
5. A. J. Bardin, R. Visintin, A. Amon, *Cell* **102**, 21 (2000).
6. A. Bloecher, G. M. Venturi, K. Tatchell, *Nature Cell Biol.* **2**, 556 (2000).
7. G. Pereira et al., *Mol. Cell* **6**, 1 (2000).
8. Cell culture and coverslip coatings were performed as described (10).
9. M. Paintrand, M. Moudjou, H. Delacroix, M. Bornens, *J. Struct. Biol.* **108**, 107 (1992).
10. M. Piel et al., *J. Cell Biol.* **149**, 317 (2000).
11. Web material is available at [www.sciencemag.org/cgi/content/full/291/5508/1550/DC1](http://www.sciencemag.org/cgi/content/full/291/5508/1550/DC1).
12. Time-lapse recordings were performed as described (10). To record post-anaphase movements of the centriole, we acquired a z-series every 2 min with a  $\times 100$  objective in both phase contrast and epifluorescence, enabling us to follow centriole movements and intercellular bridge morphology at a high resolution without losing the focus, which was crucial for determining the rupture of the bridge. The illumination device was a 100-W halogen lamp, with the potentiometer set under 8 V to avoid overillumination. In these conditions, cells could enter mitosis and exit metaphase without any delay, as compared to cells recorded in phase contrast only.
13. B. Byers, D. H. Abramson, *Protoplasma* **66**, 413 (1968).
14. J. M. Mullins, J. J. Bieseke, *Tissue Cell* **5**, 47 (1973).
15. ———, *J. Cell Biol.* **73**, 672 (1977).
16. A. Maniatis, M. Schliwa, *Cell* **67**, 495 (1991).
17. Y. Bobinac et al., *J. Cell Biol.* **143**, 1575 (1998).
18. E. H. Hinchcliffe, F. J. Miller, M. Cham, A. Khodjakov, G. Sluder, *Science* **291**, 1547 (2001).
19. A. Debec, *Nature* **274**, 255 (1978).
20. ———, C. Abbadie, *Biol. Cell* **67**, 307 (1989).
21. K. Burton, D. L. Taylor, *Nature* **385**, 450 (1997).
22. C. B. O'Connell, S. P. Wheatley, S. Ahmed, Y. L. Wang, *J. Cell Biol.* **144**, 305 (1999).
23. J. H. Zang et al., *Mol. Biol. Cell* **8**, 2617 (1997).
24. Y. Yasui et al., *J. Cell Biol.* **143**, 1249 (1998).
25. K. Emoto, M. Umeda, *J. Cell Biol.* **149**, 1215 (2000).
26. A. F. Straight, C. M. Field, *Curr. Biol.* **10**, 760 (2000).
27. J. C. Canman, D. B. Hoffman, E. D. Salmon, *Curr. Biol.* **10**, 611 (2000).
28. S. P. Wheatley, Y. Wang, *J. Cell Biol.* **135**, 981 (1996).
29. Mitotic cells were shaken off and seeded on coverslips. The coverslips were either uncoated (for HeLa cells) or coated with low (1  $\mu\text{g/ml}$  solution) or high (20  $\mu\text{g/ml}$  solution) fibronectin concentration (10). Every 30 min, cells were treated with 5  $\mu\text{M}$  ND for 15 min, fixed, and processed for immunofluorescence as described (10).
30. S. P. Wheatley et al., *J. Cell Biol.* **138**, 385 (1997).
31. C. M. Whitehead, J. B. Rattner, *J. Cell Sci.* **111**, 2551 (1998).
32. We thank A. Debec for the kind gift of the 1182-4 cell line; N. Delgehr for the tubulin-GFP-expressing U2OS cell line; and A.-M. Tassin, A. Paoletti, A. Taddei, O. Smrzka, and G. Almouzni for critical reading of the manuscript. This work was supported by CNRS and Institut Curie and by an NIH grant (to G. Sluder, University of Massachusetts Medical School, Worcester, MA).

9 November 2000; accepted 16 January 2001

## Structure of a Bag/Hsc70 Complex: Convergent Functional Evolution of Hsp70 Nucleotide Exchange Factors

Holger Sondermann,<sup>1</sup> Clemens Scheufler,<sup>1</sup> Christine Schneider,<sup>1</sup> Jörg Höfeld,<sup>2</sup> F.-Ulrich Hartl,<sup>1</sup> Ismail Moarefi<sup>1\*</sup>

Bag (Bcl2-associated athanogene) domains occur in a class of cofactors of the eukaryotic chaperone 70-kilodalton heat shock protein (Hsp70) family. Binding of the Bag domain to the Hsp70 adenosine triphosphatase (ATPase) domain promotes adenosine 5'-triphosphate-dependent release of substrate from Hsp70 in vitro. In a 1.9 angstrom crystal structure of a complex with the ATPase of the 70-kilodalton heat shock cognate protein (Hsc70), the Bag domain forms a three-helix bundle, inducing a conformational switch in the ATPase that is incompatible with nucleotide binding. The same switch is observed in the bacterial Hsp70 homolog DnaK upon binding of the structurally unrelated nucleotide exchange factor GrpE. Thus, functional convergence has allowed proteins with different architectures to trigger a conserved conformational shift in Hsp70 that leads to nucleotide exchange.

The evolutionary conserved members of the Hsp70 family play essential roles in preventing misfolding and aggregation of newly synthesized or unfolded proteins (1–3). Coordinated binding and release of substrates by these molecular chaperones is strictly dependent on their ATPase activity. Nucleotide

binding to the NH<sub>2</sub>-terminal ATPase domain of Hsp70 regulates the substrate binding properties of its COOH-terminal peptide-binding domain by an unknown mechanism (4, 5). Hsp70 binds adenosine 5'-triphosphate (ATP) with high affinity and slowly hydrolyzes it to adenosine 5'-diphosphate (ADP). ATP-bound Hsp70 has low affinity for substrate, whereas the ADP-bound form has high affinity. Substrate binding to Hsp70/ATP stimulates ATP hydrolysis (6), resulting in a more stable complex of Hsp70/ADP with bound substrate. ATP hydrolysis is also stimulated by Hsp40 proteins, an evolutionary

<sup>1</sup>Department of Cellular Biochemistry, Max-Planck-Institut für Biochemie, D-82152 Martinsried, Germany. <sup>2</sup>Institut für Zellbiologie, Rheinische Friedrich-Wilhelms-Universität Bonn, D-53121 Bonn, Germany.

\*To whom correspondence should be addressed. E-mail: ismail@moarefi.com

REPORTS

conserved family of Hsp70 co-chaperones, which promote substrate binding to Hsp70 (7, 8). Release of substrate from the complex is dependent on the exchange of bound ADP for ATP. In prokaryotes (and mitochondria), this reaction is promoted by GrpE, a nucleotide exchange factor for the bacterial Hsp70 homolog DnaK (9–12). Given the high level of conservation of Hsp70 and Hsp40 proteins, it seems likely that the cytosol of eukaryotes would contain a GrpE homolog. However, no nucleotide exchange factor for Hsp70 has been definitively identified, although such a function has been proposed for the Bcl2-associated athanogene 1 (Bag-1) protein (13).

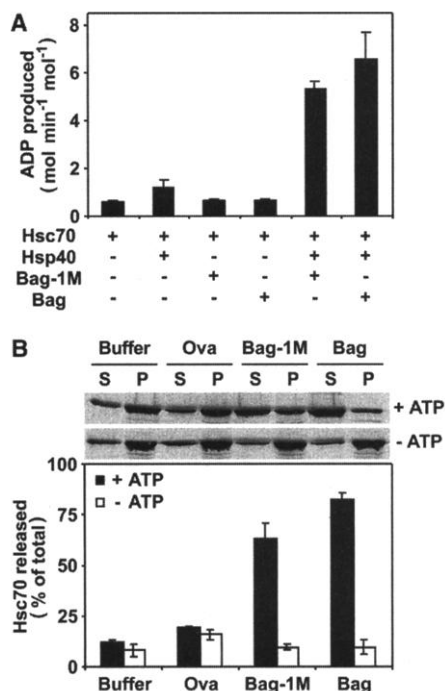


**Fig. 1.** Functional characterization of Bag-1M and the Bag domain. (A) Bag-1M and the Bag domain stimulate the ATPase activity of Hsc70 in a Hsp40-dependent manner. Hsc70 (3  $\mu$ M) was incubated at 30°C with Hsp40 (3  $\mu$ M) and Bag-1M or isolated Bag domain (3  $\mu$ M) as indicated. The amount of ATP hydrolyzed was quantitated (9, 25). (B) Bag-1M and the Bag domain stimulate Hsc70 release from substrate polypeptide in a nucleotide-dependent manner. Release of <sup>35</sup>S-methionine-labeled Hsc70 from partially denatured immobilized LBD of the glucocorticoid receptor was measured upon incubation with ovalbumin (Ova), Bag-1M, or Bag domain (5  $\mu$ M each) for 10 min at 25°C in the presence or absence of ATP/Mg<sup>2+</sup> (2 mM) (26, 33). S, supernatant fractions containing released Hsc70; P, pellet fractions containing LBD-bound Hsc70. Supernatants and pellets were analyzed by SDS-polyacrylamide gel electrophoresis, followed by phosphorimaging. The bar diagram shows the amounts of Hsc70 released from LBD expressed in percentage of total bound Hsc70. Error bars in (A) and (B) indicate SD of three independent experiments.

Bag-1 was first identified in the mammalian cytosol by virtue of its interaction with the anti-apoptotic protein Bcl-2 and was shown to promote cell survival (14). The Bag family is characterized by the Bag domain that mediates direct interaction with the Hsp70 ATPase domain (15, 16) and directly interacts with a number of client proteins, including the protein kinase Raf-1 (17), growth factor receptors (18), and the retinoic acid receptor (19). All Bag-1 isoforms (S, M, and L) contain a ubiquitin homology domain, thought to contact the proteasome (20). Bag-3 lacks the ubiquitin homology domain but contains a WW domain (W, Trp) (21). These unique sequence elements likely target individual Bag family members to their unique partners and reflect their specific roles in different cellular processes such as protein folding and degradation, signal transduction, and apoptosis. Bag-1 was shown to stimulate the ATPase rate of Hsp70 in an Hsp40-dependent manner and to promote substrate release from the chaperone. These findings led to the proposal that Bag-1 is a nucleotide exchange factor for Hsp70 (13), a view that has been controversially discussed (22).

The minimal Bag domain of Bag-1 was identified by limited proteolysis [residues 151–264 of Bag-1M (Web fig. 1) (23)]. This

construct has the same affinity for Hsc70 (the constitutively expressed cytosolic isoform of Hsp70) or its ATPase domain as the Bag isoform Bag-1M [dissociation constant  $K_d$  1 to 3  $\mu$ M; measured by isothermal titration calorimetry (Web table 1) (23)]. Binding affinity is substantially reduced in the presence of ADP or ATP, matching the characteristics of the full-length proteins (24). Hsp40-dependent ATP hydrolysis by Hsc70 is stimulated 10-fold in the presence of the Bag domain or Bag-1M (Fig. 1A) (25), and both the Bag domain and Bag-1M trigger efficient release of radiolabeled Hsc70 from a model substrate [partially denatured glucocorticoid receptor ligand binding domain (LBD)] (26) (Fig. 1B). Bag-dependent dissociation of the Hsc70/LBD complex requires the presence of ATP; binding of Bag-1 to Hsc70 alone does not trigger substrate release (Fig. 1B). Taken together, the Bag domain used for crystallization is fully functional and accounts for the effects of Bag-1M on Hsp70 activity.

We determined the crystal structure of the Bag domain in complex with the ATPase domain of Hsc70 at 1.9 Å resolution (Table 1) (27). The Bag domain forms a three-helix bundle (Fig. 2A). Helices 2 and 3 contact subdomains IB and IIB of the ATPase (Fig. 2, A and B). Binding of the monomeric Bag

**Table 1.** Data collection, phasing, and refinement statistics. Data collection values are as defined in the program SCALEPACK (34), the MAD phasing values are as defined in the program SOLVE (35), and the model refinement values are as defined in the program CNS (37). In data from the DESY x-ray source, Bijvoet pairs have been separated.

Parameter	Data collection values			
	Native	SeMet		
Space group	C2			
Unit cell	$a = 116.57 \text{ \AA}, b = 40.78 \text{ \AA}, c = 129.26 \text{ \AA}$ $\alpha = \gamma = 90^\circ, \beta = 114.84^\circ$			
No. of complexes/asymmetric unit	1			
X-ray source	ESRF, ID14-4	DESY, BW6		
Wavelength (Å)	$\lambda = 0.9287$	$\lambda_1 = 0.9786$ (peak)	$\lambda_2 = 0.9792$ (inflection)	$\lambda_3 = 0.9500$ (remote)
Resolution (Å)	15 to 1.95 (2 to 1.95)	18 to 2.6 (2.67 to 2.60)	18 to 2.6 (2.67 to 2.60)	18 to 2.6 (2.67 to 2.60)
$I/\sigma_I$	21.0 (3.6)	16.7 (5.9)	17.6 (7.0)	12.8 (7.0)
Completeness (%)	99.5 (99.6)	98.2 (97.8)	98.1 (97.4)	98.1 (97.7)
$R_{sym}$ (%)	5.6 (27.0)	3.3 (10.5)	3.2 (9.6)	3.2 (9.0)
<i>MAD phasing</i>				
Anomalous scatterer	Selenium (6 of 6 sites)			
Resolution (Å)	18 to 2.6			
Figure of merit	0.59			
<i>Model refinement</i>				
Resolution (Å)	15 to 1.9			
No. of reflections $R_{work}/R_{free}$	40,599/3,149			
$R_{work}/R_{free}$ (%)	23.4/27.9			
No. of solvent molecules	359			
rmsd bond length (Å)	0.01			
rmsd angles (degrees)	1.4			

\*No  $\sigma$  cutoffs.

REPORTS

domain to the ATPase domain is mediated by electrostatic interactions, mainly exploiting residues Glu<sup>212</sup>, Asp<sup>222</sup>, Arg<sup>237</sup>, and Gln<sup>245</sup> in Bag-1 (Fig. 2C). These residues are highly conserved in all known Bag proteins, and their individual replacement with alanine results in Bag variants with substantially decreased activity in ATPase and substrate release assays, consistent with reduced affinities for the Hsc70 ATPase domain (28). A structure-based sequence search reveals Bag proteins in the cytosol of all eukaryotic species (Fig. 2D). The main residues of Hsc70 involved in the interaction are Arg<sup>261</sup> and Glu<sup>283</sup>. All Hsc70 residues involved in the interaction with Bag (Fig. 2C) are absolutely conserved in all cytosolic forms of eukaryotic Hsp70 proteins, correlating with the occurrence of Bag proteins in the cytosol, but are highly divergent in DnaK and BiP (the Hsp70 paralog in the endoplasmic reticulum), proteins that either rely on GrpE as a nucleotide exchange factor (DnaK) or are thought to

function independently of an exchange factor (BiP).

Although the Bag domain and GrpE of

*Escherichia coli* are structurally unrelated (Fig. 3, A and B), they interact with the same subdomains, IB and IIB, of their respective

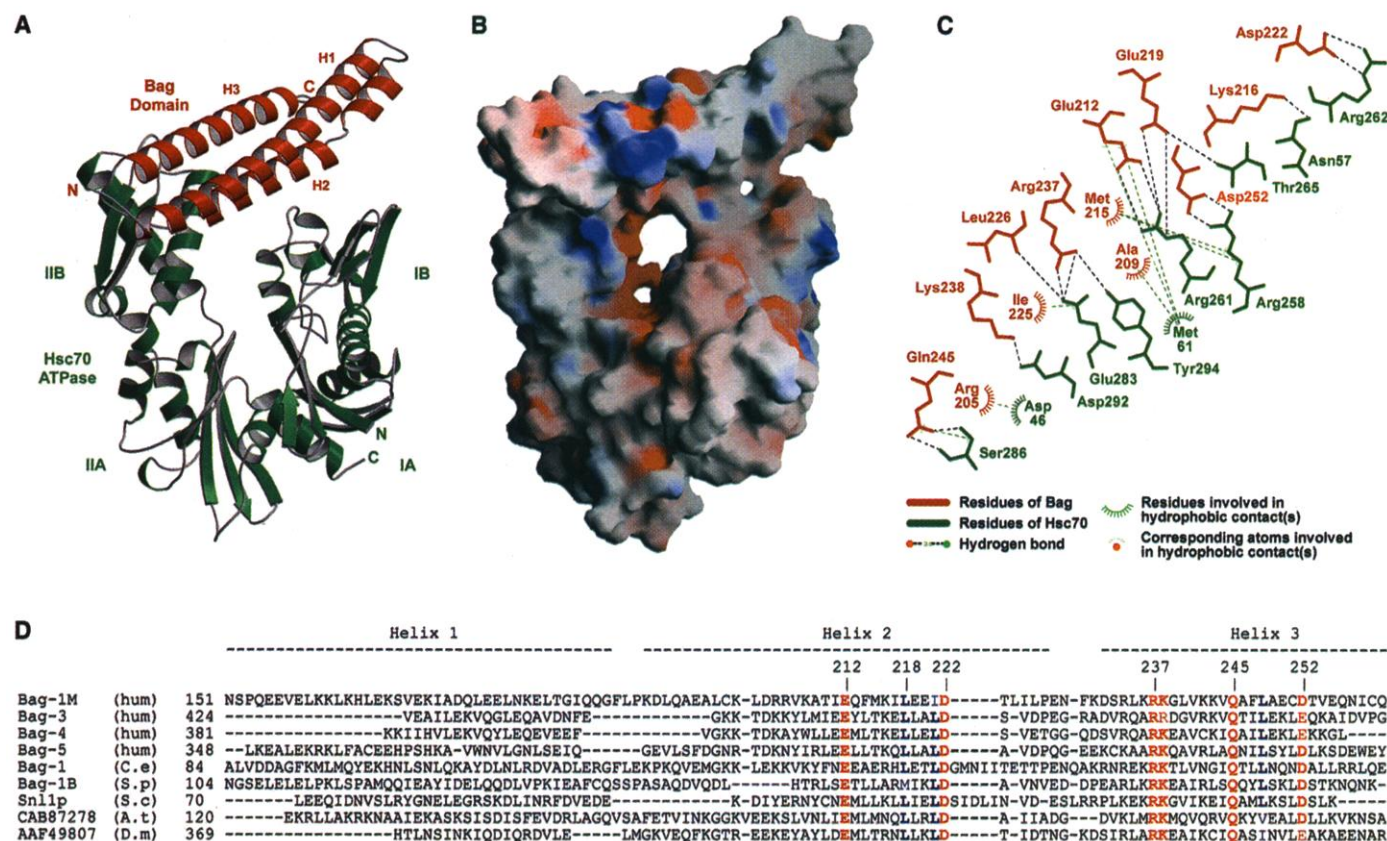


**Fig. 2.** The Bag domain/Hsc70 complex. (A) The backbones of the Bag domain (red) and the ATPase domain of Hsc70 (green) shown in a ribbons representation generated with the program Bobscrip (38). (B) The electrostatic potential of the Bag domain/Hsc70 (residues 5–381) complex modeled onto the accessible molecular surface as calculated and visualized with GRASP (39). Red and blue indicate negative and positive charges, respectively. Orientation as in (A). (C) Schematic diagram of the interactions between Hsc70 and the Bag domain. The diagram was produced by LIGPLOT (40). Red, residues of Bag-1M; green, residues of Hsc70. (D) Structure-based sequence alignment of Bag do-

main proteins from different species. Conserved residues forming the interaction surface with the Hsc70 ATPase domain are highlighted in red, and residues important for packing interactions are shown in blue (41). GenBank accession numbers are as follows: human Bag-1M human (hum), Q99933; human Bag-3/CAIR/BIS, AAD16122; human Bag-4, AAD16123; human Bag-5, AAD16124; *Caenorhabditis elegans* (C.e) Bag-1, AAD16125; *Schizosaccharomyces pombe* (S.p) Bag-1B, AAD16127; *Saccharomyces cerevisiae* (S.c) Sn1lp, NP\_012248; *Arabidopsis thaliana* (A.t) putative protein, CAB87278; and *Drosophila melanogaster* (D.m) gene product, AAF49807.

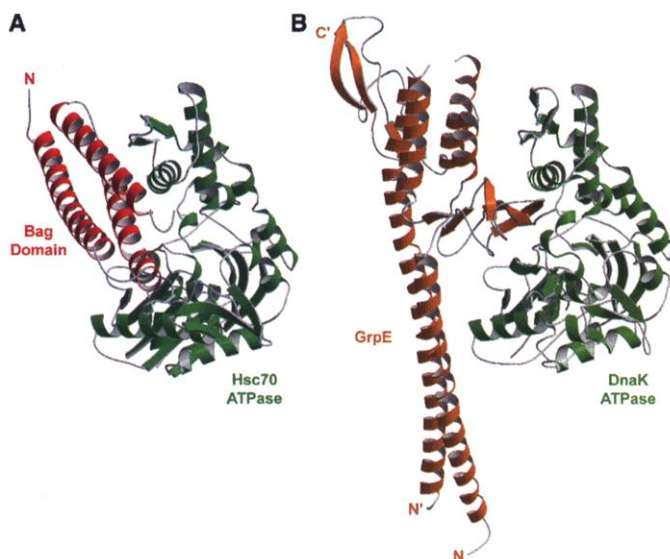


**Fig. 3.** Structural comparison of (A) Bag domain/Hsc70 and (B) DnaK/GrpE complexes. The ATPase domains of Hsc70 and DnaK are colored green, the Bag domain is red, and GrpE is yellow.

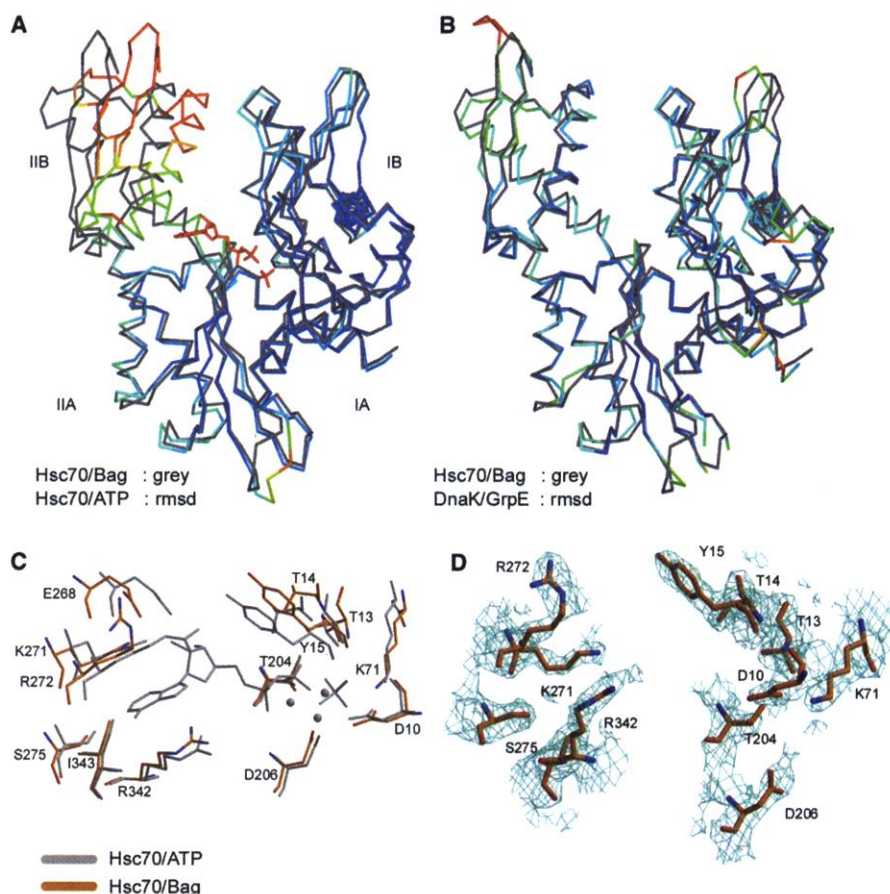


**Fig. 4.** Nucleotide exchange mechanism of Bag and GrpE proteins. **(A and B)** Superposition of Hsc70 (residues 5–381) in complex **(A)** with the Bag domain with the nucleotide-bound domain of Hsc70 (PDB code 3Hsc) and **(B)** with the ATPase domain of DnaK in complex with its nucleotide exchange factor GrpE (PDB code 1DKG). Color code represents the rmsd of the superpositions calculated and visualized by the SwissPDB Viewer (blue, low degree of deviation; red, high degree of deviation). A loop region in domain IIB of DnaK not present in Hsc70 is shown in red (maximal rmsd). **(C)** Superposition of the side chains in Hsc70 involved in ATP binding and hydrolysis. The nucleotide-bound state is drawn in gray; the conformation of the respective residues in the Bag domain/Hsc70 (residues 5–381) complex is drawn in orange (41). **(D)** A  $2F_o - F_c$  simulated annealing omit map of the Hsc70 region involved in ATP binding and hydrolysis calculated in the absence of the indicated residues (contour level at  $1\sigma$ ) (41).

Hsp70 ATPase domain. However, in contrast to the Bag domain, GrpE forms a dimer that mainly employs a  $\beta$  strand subdomain, in addition to contacts from its  $\alpha$  helical region, to bind to the ATPase domain of DnaK (Fig. 3B) (12). Hydrophobic contacts from the  $\beta$  strand region of GrpE reach deep into the nucleotide-binding cleft and contribute substantially to the tight interaction of the two proteins. Different residues are contacted in the Hsp70 ATPase domains of the two complexes. GrpE also interacts with a loop in DnaK that is not conserved in eukaryotic cytosolic forms of Hsp70 (Fig. 4B).

The consequence of Bag-1 binding to the Hsp70 ATPase domain is a  $14^\circ$  rotation of subdomain IIB about a hinge in the region of Leu<sup>228</sup> and Leu<sup>309</sup> relative to the structure of Hsc70 with bound ATP [Fig. 4A and Web fig. 2A (23)] (29). In this region, the highest root mean square deviation (rmsd) between the two structures is

observed [Web fig. 3 (23)]. Despite striking structural differences between the Bag domain and GrpE, the conformation of the Hsc70 ATPase in complex with Bag is remarkably similar to the conformation of the ATPase domain of DnaK in complex with GrpE [Fig. 4B and Web fig. 2B (23)] (12). In both cases, this conformation is incompatible with high-affinity nucleotide binding. Thus, the eukaryotic Bag domain has evolved convergently to induce a nucleotide release mechanism that has been conserved in Hsp70 proteins.

The high-resolution crystal structure allows the analysis of the conformational changes in positions that are critical for nucleotide binding and hydrolysis by superimposing relevant residues from Hsc70 bound to ATP (29) and Hsc70 bound to Bag [Fig. 4C and Web fig. 4 (23)]. The main changes in the ATPase domain induced by binding of the Bag domain occur in residues of subdo-

main IA and IIB that orient the adenosine moiety of the nucleotide. The positions of other residues in the binding cleft and the residues involved in catalysis of ATP hydrolysis in subdomains IB and IIA are not significantly altered. The structural transition results in a movement of Glu<sup>268</sup>, Lys<sup>271</sup>, and Ser<sup>275</sup> in domain IIB and Thr<sup>13</sup>, Thr<sup>14</sup>, and Tyr<sup>15</sup> in subdomain IA away from their position in the nucleotide-bound structure. This leads to an opening of the nucleotide-binding cleft. Additionally, the side chain of Arg<sup>272</sup> assumes an alternative conformation when compared to the nucleotide-bound state. In the latter state, Arg<sup>272</sup> and Arg<sup>342</sup> form a clamp that fixes the adenine ring through hydrophobic interactions and the  $\pi$ -electron system of their guanidinium groups.

The Bag domain promotes nucleotide release from Hsp70 by opening the nucleotide-binding cleft upon binding to the ADP-bound state of Hsp70. Because of the excess of ATP over ADP and Bag proteins in the eukaryotic cytosol, ATP will enter the nucleotide-binding pocket and displace bound Bag protein, resulting in an acceleration of nucleotide exchange. In the presence of Hsp40, which stimulates ATP hydrolysis, nucleotide exchange becomes rate limiting; in the absence of Hsp40, ATP hydrolysis is rate limiting. Thus, an acceleration of the ATPase is only observed in the presence of both Hsp40 and Bag-1 (Fig. 1, B and C). The nucleotide binding and release kinetics of the ATPase cycle are almost identical for Hsp70 and DnaK (10, 30, 31). Given the strict dependence of DnaK on an efficient nucleotide exchange factor, it seems likely that a nucleotide exchange factor is necessary for at least some Hsp70 functions in the eukaryotic cytosol, as supported by the occurrence of Bag proteins in all eukaryotes.

On the basis of our structural analysis, it is clear that Bag proteins function as nucleotide exchange factors for Hsp70 by stabilizing the nucleotide-free state of the ATPase. A similar mechanism has been described for the protein Sos, the nucleotide exchange factor of the guanosine triphosphatase Ras (32). In both cases, efficient release and rebinding of nucleotides are achieved by a conformational change that is induced in the enzyme by insertion of two  $\alpha$  helices from the exchange factor into the nucleotide-binding cleft.

Bag and GrpE represent two nucleotide exchange factors for Hsp70 proteins with different structures that have been optimized through functional conversion. By binding to different regions of their partner proteins, both GrpE and the Bag domain trigger a conserved switch in the Hsp70 ATPase domain. It remains to be established whether this conserved switch is exploited by yet unidentified additional exchange factors.

References and Notes

1. B. Bukau, E. Deuerling, C. Pfund, E. A. Craig, *Cell* **101**, 119 (2000).
2. B. Bukau, A. L. Horwich, *Cell* **92**, 351 (1998).
3. F. U. Hartl, *Nature* **381**, 571 (1996).
4. D. R. Palleros, K. L. Reid, L. Shi, W. J. Welch, A. L. Fink, *Nature* **365**, 664 (1993).
5. M. Pellicchia *et al.*, *Nature Struct. Biol.* **7**, 298 (2000).
6. G. C. Flynn T. G. Chappell, J. E. Rothman, *Science* **245**, 385 (1989).
7. D. M. Cyr, X. Lu, M. G. Douglas, *J. Biol. Chem.* **267**, 20927 (1992).
8. J. S. McCarty, A. Buchberger, J. Reinstein, B. Bukau, *J. Mol. Biol.* **249**, 126 (1995).
9. K. Liberek, D. Skowrya, M. Zyllicz, C. Johnson, C. Georgopoulos, *Proc. Natl. Acad. Sci. U.S.A.* **88**, 2874 (1991).
10. L. Packschies *et al.*, *Biochemistry* **36**, 3417 (1997).
11. A. Szabo *et al.*, *Proc. Natl. Acad. Sci. U.S.A.* **91**, 10345 (1994).
12. C. J. Harrison, M. Hayer-Hartl, M. Di Liberto, F.-U. Hartl, J. Kuriyan, *Science* **276**, 431 (1997).
13. J. Höhfeld, S. Jentsch, *EMBO J.* **16**, 6209 (1997).
14. S. Takayama *et al.*, *Cell* **80**, 279 (1995).
15. S. Takayama *et al.*, *EMBO J.* **16**, 4887 (1997).
16. M. Zeiner, M. Gebauer, U. Gehring, *EMBO J.* **16**, 5483 (1997).
17. H.-G. Wang, S. Takayama, U. R. Rapp, J. C. Reed, *Proc. Natl. Acad. Sci. U.S.A.* **93**, 7063 (1996).
18. A. Bardelli *et al.*, *EMBO J.* **15**, 6205 (1996).
19. R. Liu *et al.*, *J. Biol. Chem.* **273**, 16985 (1998).
20. J. Lüders, J. Demand, J. Höhfeld, *J. Biol. Chem.* **275**, 4613 (2000).
21. S. Takayama, Z. Xie, J. C. Reed, *J. Biol. Chem.* **274**, 781 (1999).
22. D. Bimston *et al.*, *EMBO J.* **17**, 6871 (1998).
23. Supplemental Web material is available at [www.sciencemag.org/cgi/content/full/291/5508/1553/DC1](http://www.sciencemag.org/cgi/content/full/291/5508/1553/DC1).
24. J. K. Stuart *et al.*, *J. Biol. Chem.* **273**, 22506 (1998).
25. We determined ATP hydrolysis rates as described (9), using 3  $\mu$ M Hsc70 purified from bovine brain in the presence or absence of 3  $\mu$ M Hsp40, Bag-1M, or Bag domain, as indicated in Fig. 1C.
26. Hsc70 release from substrate was measured as described (33).
27. Bovine Hsc70 ATPase (residues 5–381, identical to the human homolog) and Bag domain (residues 151–363 of human Bag-1M) were produced as His<sup>6</sup>-tagged proteins in *E. coli*. A selenomethionine (Se-Met)-labeled derivative of the ATPase domain was produced in the *E. coli* strain B834(DE3). After chromatography on NiNTA (Qiagen, Valencia, CA), the His<sup>6</sup>-tag of the Bag domain was removed by using tobacco etch virus (TEV) protease. A stable, nucleotide-free complex with a 1:1 stoichiometry [see Web table 1 (23)] was purified to homogeneity by chromatography on Resource Q (Pharmacia), followed by gel filtration. Crystals were grown at 20°C in hanging drops by mixing equal volumes of protein complex [40 mg/ml in 10 mM Hepes (pH 7.5)] and reservoir solution [50 to 100 mM K-Na-tartrate, 12 to 16% polyethylene glycol (average molecular weight of 3350), 0.1 M tris (pH 8.5), and 25% (w/v) glycerol]. Crystals were flash-cooled in liquid nitrogen and kept at 100 K during data collection at beamlines ID14-4 [European Synchrotron Radiation Facility (ESRF), Grenoble, France], for native data, and BW6B [Deutsches Elektronen-Synchrotron (DESY), Hamburg, Germany], for multiple anomalous dispersion (MAD) data. Data sets were processed with the HKL software package (34). Structure solution was achieved by MAD phasing techniques with the program SOLVE (35). After solvent correction with the program DM (36), the known structure of the ATPase domain of Hsc70 was placed into the electron density, and the structure of the Bag domain was built manually. The structure was refined with the program CNS (37). The somewhat high  $R_{free}$  of the final model can in part be attributed to significant radiation damage during the collection of the native data set that could only be partially corrected during data processing and scaling. The His<sup>6</sup> tag of the Hsc70 ATPase was completely disordered and is not included in the final

- model. Upon crystallization, a disulfide bridge between Cys<sup>259</sup> at the COOH-terminus of the Bag domain and Cys<sup>201</sup> was formed. However, binding of the Bag domain to Hsc70 was not affected by reducing agents.
28. H. Sondermann, unpublished data.
29. K. M. Flaherty, C. DeLuca-Flaherty, D. B. McKay, *Nature* **346**, 623 (1990).
30. J.-H. Ha, D. B. McKay, *Biochemistry* **34**, 11635 (1995).
31. H. Theyssen, H. P. Schuster, L. Packschies, B. Bukau, J. Reinstein, *J. Mol. Biol.* **263**, 657 (1996).
32. P. A. Boriack-Sjodin, S. M. Margarit, D. Bar-Sagi, J. Kuriyan, *Nature* **394**, 337 (1998).
33. J. C. Young, F. U. Hartl, *EMBO J.* **19**, 5930 (2000).
34. Z. Otwinowski, W. Minor, *Methods Enzymol.* **276**, 307 (1997).
35. T. C. Terwilliger, J. Berendzen, *Acta Crystallogr.* **D55**, 849 (1999).
36. Collaborative Computational Project Number 4, *Acta Crystallogr.* **D50**, 760 (1994).

37. A. T. Brünger *et al.*, *Acta Crystallogr.* **D54**, 905 (1998).
38. R. M. Esnouf, *Acta Crystallogr.* **D55**, 938 (1999).
39. A. Nicholls, R. Bharadwaj, B. Honig, *Biophys. J.* **64**, A166 (1993).
40. A. C. Wallace, R. A. Laskowski, J. M. Thornton, *Protein Eng.* **8**, 127 (1995).
41. Single-letter abbreviations for the amino acid residues are as follows: A, Ala; C, Cys; D, Asp; E, Glu; F, Phe; G, Gly; H, His; I, Ile; K, Lys; L, Leu; M, Met; N, Asn; P, Pro; Q, Gln; R, Arg; S, Ser; T, Thr; V, Val; W, Trp; and Y, Tyr.
42. We thank M. Rosenhagen for help with protein crystallization and the staff at the European Molecular Biology Laboratory and Max-Planck-Institut beamlines for their support during data collection. J.H. was supported by the Deutsche Forschungsgemeinschaft (grant Hö 1518/4-1). Protein coordinates are available from the Protein Data Bank (PDB) (code 1HX1).

8 November 2000; accepted 17 January 2001

## Taste Receptor Cells That Discriminate Between Bitter Stimuli

Alejandro Caicedo<sup>1,3\*</sup> and Stephen D. Roper<sup>1,2,4</sup>

Recent studies showing that single taste bud cells express multiple bitter taste receptors have reignited a long-standing controversy over whether single gustatory receptor cells respond selectively or broadly to tastants. We examined calcium responses of rat taste receptor cells in situ to a panel of bitter compounds to determine whether individual cells distinguish between bitter stimuli. Most bitter-responsive taste cells were activated by only one out of five compounds tested. In taste cells that responded to multiple stimuli, there were no significant associations between any two stimuli. Bitter sensation does not appear to occur through the activation of a homogeneous population of broadly tuned bitter-sensitive taste cells. Instead, different bitter stimuli may activate different subpopulations of bitter-sensitive taste cells.

Recently, a large family of bitter taste receptors was identified in humans and rodents (1, 2). Although individual receptors were shown to respond selectively to a particular compound (3), taste cells expressed mRNAs for several receptors (1, 2). The findings were interpreted as showing that individual taste cells respond to several different compounds (1). However, behavioral and physiological studies in humans, monkeys, and rats indicate that bitter stimuli can be discriminated (4–8). Whether taste cells respond specifically to certain bitter stimuli is an unresolved issue. Unfortunately, our understanding of whether taste cells respond to multiple bitter compounds has depended on inferences from indirect studies [expression patterns of receptor mRNA (1, 2) and recordings from

the afferent nerve (7) and cortical neurons (8)]. Here, we used Ca<sup>2+</sup> imaging to measure direct activation of taste cells in situ to investigate how bitter taste stimuli are detected in taste buds (9). With this method, it is possible to view single taste cells in foliate slices in situ with a confocal microscope and record Ca<sup>2+</sup> changes in intact taste buds (9–11) (Fig. 1). A series of representative compounds widely used in studies of bitter taste was selected for this study at concentrations that elicit behavioral responses in rats (12–20).

Cycloheximide (10  $\mu$ M) induced large transient intracellular Ca<sup>2+</sup> increases in foliate taste cells that showed little if any adaptation or desensitization [mean peak amplitude of the relative fluorescence change  $\Delta F/F$ , 46.6  $\pm$  6.5% (Fig. 2)]. This contrasts with the pronounced adaptation reported for the expressed murine cycloheximide receptor (3). Lowering extracellular Ca<sup>2+</sup> concentration did not reduce cycloheximide responses in the cell bodies (Fig. 2D) (21) or apical processes. None of the cells that responded to cycloheximide

<sup>1</sup>Department of Physiology and Biophysics, <sup>2</sup>Program in Neuroscience, University of Miami School of Medicine, 1600 NW 10th Avenue, Miami, FL 33136, USA.

<sup>3</sup>Laboratorio de Biofísica, Centro Internacional de Física, AA 49480, Bogotá, Colombia. <sup>4</sup>Rocky Mountain Taste and Smell Center, Denver, CO 90262, USA.

\*To whom correspondence should be addressed. E-mail: [acaicedo@chroma.med.miami.edu](mailto:acaicedo@chroma.med.miami.edu)